1   **Cobomarsen, an oligonucleotide inhibitor of miR-155, slows DLBCL tumor cell growth *in***

2   ***vitro* and *in vivo***

3

4   Eleni Anastasiadou[1,5], Anita G. Seto[2], Xuan Beatty[2], Melanie Hermreck[2], Maud-Emmanuelle

5   Gilles[1], Dina Stroopinsky[3], Lauren C. Pinter-Brown[4], Linda Pestano[2], Cinzia Marchese[5], David

6   Avigan[3], Pankaj Trivedi[5], Diana Escolar[2], Aimee L. Jackson[2] and Frank J Slack*[1]

7

8   1: HMS Initiative for RNA Medicine, Department of Pathology, Beth Israel Deaconess Medical

9   Center, Harvard Medical School, Boston, MA USA.

10   2: miRagen Therapeutics, Inc, Boulder, CO, USA.

11   3: Department of Hematology, Beth Israel Deaconess Medical Center, Harvard Medical School,

12   Boston, MA USA.

13   4: Department of Internal Medicine, Division of Hematology/Oncology, University of

14   California, Irvine, CA USA

15   5: Department of Experimental Medicine, Sapienza University of Rome, Italy

16

17   **Running title:** Cobomarsen, a miRNA-based compound for DLBCL treatment

18   **Keywords:** miR-155, DLBCL, miRNA-based cancer therapy, oncomiR, lymphoma

19

20   *Corresponding Author: Frank J. Slack, Beth Israel Deaconess Medical Center,

21   330 Brookline Ave, Boston, MA 02215. Phone: 617-735-2601; Fax: 617-735-2646;

22   E-mail: fslack@bidmc.harvard.edu

23

28   **Word count of the main text:** 4958

29   **Total number of figures and tables:** Figures:6, Tables:2

30 **Statement of translational relevance**

31 Our *in vitro* and *in vivo* preclinical studies recapitulate the important role of miR-155 in the

32 pathogenesis of Diffuse Large B-cell Lymphoma (DLBCL) and in particular of the most

33 aggressive and hard-to-treat non-Germinal Center B-cell subtype DLBCL also called activated

34 B-cell subtype of DLBCL (non-GC/ABC-DLBCL). Cobomarsen, an anti-miR-155 compound,

35 effectively inhibited proliferation and induced apoptosis in ABC-DLBCL cell lines with high

36 endogenous miR-155 expression and reduced tumor growth in xenografts. Most importantly,

37 administration of this compound in a DLBCL patient who was resistant to all previous

38 therapeutic regimens, provided new insights for the safety and therapeutic potential of

39 cobomarsen monotherapy for management of patients with refractory ABC-DLBCL.

40 Cobomarsen-based therapy could be extended not only to ABC-DLBCLs but also to other types

41 of lymphomas characterized by high miR-155 expression, either as a single agent or in

42 combination with other therapeutic regimens.

43

44

45

46

47

48

49

50

51

52

53

54 **Abstract**

55 **Purpose:** MicroRNA-155, is an oncogenic miRNA, highly expressed in B-cell malignancies,

56 particularly in the non-Germinal Center B-cell or activated B-cell subtype of Diffuse Large B-

57 cell Lymphoma (non-GCB/ABC-DLBCL), where it is considered a potential diagnostic and

58 prognostic biomarker. Thus, miR-155 inhibition represents an important therapeutic strategy for

59 B-cell lymphomas. In this study, we tested the efficacy and pharmacodynamic activity of an

60 oligonucleotide inhibitor of miR-155, cobomarsen, in ABC-DLBCL cell lines and in

61 corresponding xenograft mouse models. In addition, we assessed the therapeutic efficacy and

62 safety of cobomarsen in a patient diagnosed with aggressive ABC-DLBCL.

63 **Experimental design:** Pre-clinical studies included the delivery of cobomarsen to highly miR-

64 155 expressing ABC-DLBCL cell lines to assess any phenotypic changes as well as intravenous

65 injections of cobomarsen in NSG mice carrying ABC-DLBCL xenografts to study tumor growth

66 and pharmacodynamics of the compound over time. To begin to test its safety and therapeutic

67 efficacy, a patient was recruited who underwent five cycles of cobomarsen treatment.

68 **Results:** Cobomarsen decreased cell proliferation, and induced apoptosis in ABC-DLBCL cell

69 lines. Intravenous administration of cobomarsen in a xenograft NSG mouse model of ABC-

70 DLBCL reduced tumor volume, triggered apoptosis, and de-repressed direct miR-155 target

71 genes. Finally, the compound reduced and stabilized tumor growth without any toxic effects for

72 the patient.

73 **Conclusions:** Our findings support the potential therapeutic application of cobomarsen in ABC-

74 DLBCL and other types of lymphoma with elevated miR-155 expression.

75

76

77   **Introduction**

78   DLBCL accounts for approximately 30-58% of all non-Hodgkin lymphomas (NHL). Based on

79   gene expression and immunohistochemical profiling within the B-cell lineage, there are two

80   main molecular subtypes, namely the Germinal Center B-cell (GCB) derived DLBCL and the

81   non-GCB or ABC type (1,2). The incidence of the latter type is approximately 40% of all

82   DLBCL cases with higher incidence in the elderly (3,4). More recent studies have explored the

83   genomic landscape of DLBCL by whole exome, targeted amplicons, and transcriptomic

84   sequencing to specifically identify combinations of genetic changes (5,6). Through an improved

85   distinction of different genomic subgroups of DLBCLs, these two groundbreaking studies have

86   enabled improved risk stratification before the patients receive the standard chemotherapy or

87   immunotherapy. Generally, ABC-DLBCL patients have a worse prognosis, usually owing to

88   higher expression of *BCL2, BCL6* and *MYC* oncogenes (7-9). The standard treatment is a

89   cocktail of the chemotherapeutic drugs cyclophosphamide, doxorubicin, vincristine and

90   prednisone combined with rituximab monoclonal antibodies (R-CHOP), followed by radiation

91   therapy or surgery. A selective efficacy of R-CHOP in combination with ibrutinib or

92   lenalidomide has also been reported (10,11). Although chemotherapy prolongs the survival of

93   DLBCL patients, relapse and drug resistance are not uncommon and may occur in as many as

94   40% of patients (12). Particularly, the complete response (CR) rate in ABC-type DLBCL

95   patients to R-CHOP chemotherapy is only 30% while a higher CR rate of 70% is observed in

96   GC-type DLBCL patients (3,13).

97

98   MicroRNAs (miRNAs) are 20-22 nucleotide long non-coding RNAs, which inhibit the

99   translation of genes that participate in a variety of biological processes including differentiation,

100   inflammation, immunity and tumorigenesis (14). Among known miRNAs involved in cancer,

101   increased miR-155 expression is crucial for B-cell lymphoma initiation and progression (15-17).

102   Thus, miR-155 has emerged as a diagnostic and prognostic marker as well as a therapeutic target

103   in B-cell malignancies including DLBCL (18,19). The primary transcript from which the mature

104   miR-155 is processed, the B-cell integration cluster (BIC), is also highly expressed in Hodgkin

105   (HL) and non-Hodgkin lymphomas (NHL) (20). In particular, the nuclear factor (NF)-κB binds

106   to the BIC promoter, and might induce miR-155 expression. Since NF-kB is constitutively

107   activated in ABC-DLBCL rather than in the GC subtype, this might explain higher miR-155

108   expression in ABC-DLBCL (21,22). Furthermore, high expression of miR-155 in E(mu)-mmu-

109   miR155 transgenic mice was sufficient to develop a lymphoproliferative disease that resembles

110   human acute lymphoblastic leukemia or high-grade lymphomas (23). MiR-155-expressing

111   lymphomas display features of oncogene addiction, epitomized in the doxycycline Tet-Off-based

112   mouse model miR-155^{LSLtTA} (24,25).

113

114   Several other *in vitro* and *in vivo* studies point to miR-155 as a *bona fide* pharmacological target

115   of miRNA-based therapy in lymphoma (18). In a recent study, inhibition of miR-155 using

116   cobomarsen in cutaneous T-cell lymphoma (CTCL) cell lines de-repressed miR-155 target genes,

117   decreased proliferation and induced apoptosis (26). Based in part on these results, cobomarsen is

118   being assessed in a phase II clinical trial for the treatment of CTCL, mycosis fungoides subtype

119   (MF-CTCL), (https://clinicaltrials.gov/ct2/show/study/NCT03713320).

120

121   Over the years, it has become apparent that miR-155 may represent a therapeutic target

122   especially in the ABC-type DLBCL, where the estimated CR rate to conventional therapeutic

123   management is still very low, underlining the importance of developing novel therapeutic

124   strategies (12). Given the role of miRNA deregulation in cancer and particularly of miR-155 in

125   DLBCLs, in the present study, we investigated the effect of cobomarsen in ABC-DLBCL cell

126   lines with high miR-155 expression (27). Additionally, *in vivo* efficacy of cobomarsen was tested

127   in xenografts and in a patient with aggressive DLBCL.

128

129   **Materials and methods**

130

131   **Cells:** ABC-type DLBCL cell lines, U2932, OCI-LY3 and RCK8 were purchased from DSMZ

132   and were grown in a RPMI1640 medium supplemented with 10% FBS without antibiotics and

133   kept in a 37C, 5% CO2 incubator. All cell lines were mycoplasma free tested with MycoAlert™

134   mycoplasma detection kit (LONZA). ABC-type DLBCL cell lines were chosen because of their

135   high miR-155 expression, compared to normal CD19+ B cells.

136

137   **Oligonucleotide**: Cobomarsen is a single-stranded, chemically-modified miR-155 targeting

138   oligonucleotide. Cobomarsen and its corresponding fluorescein isothiocyanate (FITC)

139   conjugated variant were synthesized and purified by miRagen Therapeutics (Boulder, CO, USA).

140   A *Caenorhabditis elegans* anti-miRNA that does not target any mammalian microRNA is used

141   throughout as control oligonucleotide (26).

142

143   **Quantitative RT-PCR (qRT-PCR):** Total RNA was isolated from 3×10^6 cells from each cell

144   line using Direct-zol RNA MiniPrep Plus kit (Zymo Research) according to manufacturer's

145   instructions. We used commercially available Human B Cell (CD19+) total RNA isolated from

146 highly purified human CD19+ B lymphocytes, derived from multiple healthy donors (Miltenyi

147 biotec Inc. Cat.n. 130-093-169). The integrity of RNA was routinely checked using 1% agarose

148 gel and RNA quantification was estimated with a DS-11 spectrophotometer (DeNovix).

149 Synthesis of cDNA was performed by retro-transcribing 1µg RNA with SuperScript® IV First-

150 Strand Synthesis System (Invitrogen) according the manufacturer's instructions. For miR-155

151 detection, 1µg RNA was retro-transcribed with miScriptII RT kit (QIAGEN).

152 RNA extraction from mice xenografts was performed using the RNeasy Plus 96 Kit, (Qiagen, cat

153 # 74192) according to the manufacturer's instructions. Nine µl of the isolated RNA were

154 subjected to reverse transcription using the High Capacity cDNA Reverse Transcription Kit,

155 (Applied Biosystems, cat# 4368813). Additional details of q-RT-PCR conditions can be found in

156 supplementary materials and methods.

157

158 **Cobomarsen delivery verification:** Two different concentrations, 2.5 and 10µM of FITC

159 conjugated cobomarsen were delivered without any transfection reagent into $5x10^4$ U2932 cells

160 in a 12-well plate for 6 hours. Cobomarsen positive cells were detected by flow cytometry using

161 a Gallios flow analyzer (Beckman Coulter).

162 Visualization of the compound (2.5µM) in U2932 cells 48h post-delivery was performed with

163 Zeiss LSM 880 Confocal Microscope. Further details can be found in the supplementary

164 materials and methods.

165

166 **MiR-155 luciferase reporter**: To verify whether cobomarsen can suppress endogenous miR-155

167 activity, U2932, OCI-LY3 and RCK8 cells were seeded one day before transfection with

168 psiCHECK-2 miR-155 biosensor at a concentration of $2x10^5$ cells/well in triplicates in a 24-well

169 plate. 20ng psiCHECK-2 miR-155 biosensor was transfected with DharmaFECT Duo

170 Transfection Reagent (Dharmacon), as previously described (25). Twenty-four hours post-

171 transfection, culture medium was carefully removed from each well and replenished with 1.5

172 ml/well of fresh medium containing 10µM cobomarsen or 10µM control oligonucleotide and in

173 the absence of any transfection reagent. Twenty-four hours later, the relative luminescence units

174 (RLU) of miR-155 luciferase activity was detected with Dual luciferase reporter assay (Promega)

175 and recorded with GloMax explorer instrument (Promega), according to the manufacturer's

176 instructions. The experiment was repeated at least three times. Further details are in

177 supplementary materials and methods.

178

179 **Cell Proliferation assay:** Cobomarsen or oligonucleotide control transfected cells ($2x10^4$ per

180 well) were placed in triplicate, in a 96 opaque-walled flat well plates for cell culture to estimate

181 cell proliferation over time. At 48h,72h and 96h post-delivery of the compounds, 100µl of

182 CellTiter-Glo Reagent (Promega) was added in each well, according to the manufacturer's

183 instructions. The experiment was repeated at least three times. Further details are described in the

184 supplementary materials and methods.

185

186 **Apoptosis assay by AnnexinV/PI (propidium iodide**): To study whether cobomarsen has any

187 effect on apoptosis in DLBCL cell lines with high levels of miR-155, 10µM control

188 oligonucleotide or cobomarsen was added directly to 2 ml of cell culture medium containing

189 $5x10^5$ U2932, OCI-LY3 and RCK8 cells in a 6 well plate. The cell culture medium was

190 replenished with fresh medium containing the corresponding oligonucleotide at 48h to sustain

191 viability. After 96h, one million cells from each cell line were harvested, washed in PBS and

192   stained for apoptosis according to APC Annexin V Apoptosis Detection with PI Kit instructions

193   (BioLegend). Detection of the percentage of early apoptotic (only Annexin V positive), late

194   apoptotic (both Annexin V/PI positive), and necrotic cells (only PI) was performed using a

195   Gallios flow analyzer (Beckman Coulter). Data were analyzed with Kaluza for Gallios Software

196   (28). The experiment was repeated three times for each cell line.

197

198   **DLBCL xenografts in mice:** Five-to-six week old female NSG (*NOD*.Cg-Prkdc^{scid}

199   Il2rg^{tm1Wjl}/SzJ, strain n. 005557) mice were purchased from The Jackson laboratory and were

200   maintained at the BIDMC mouse facility in accordance with the Institutional Animal Care and

201   Use Committee (IACUC) guidelines. Ten million U2932 cells were injected subcutaneously

202   (s.c.) on the left flank of 54 mice included in the tumor growth and pharmacodynamic studies.

203   After 9-12 days, when the tumor volume reached a range of 100-200 mm^3, the mice were

204   randomized into groups based on the mean of their tumor volumes and the standard deviation

205   between the groups. This was done to ensure an even distribution of tumor volumes on the first

206   day of treatment. Treatments were performed through intravenous injections (i.v.) in the tail

207   vein, using a 27-gauge syringe. For the tumor growth study, a total of 24 mice were divided into

208   four treatment groups (Table 1):

209   Group A contained 12 mice treated with 100μl of phosphate buffered saline (PBS). Group B

210   contained 12 mice treated with 100μl PBS containing 1mg/ml cobomarsen. To ensure that the

211   control oligo did not have any impact on the tumor growth, group C and D contained 3 mice

212   each treated respectively with 100μl PBS and 100μl PBS contained 1mg/ml cobomarsen. For the

213   pharmacodynamic study 24 mice were divided into four groups, 8 mice each treated with 100μl

214   PBS (group 1), 1mg/kg control oligo (group 2) and 1mg/kg cobomarsen (group 3) (Table 2).

215   Tumor volume was measured with an electronic caliper at baseline and prior to each i.v.

216   injection. According to the IACUC guidelines, once the tumor volume in the control groups,

217   (PBS or control oligo groups) has reached 2000mm^3, all mice were euthanized. The number of

218   animals treated with Cobomarsen, control oligonucleotide or vehicle/PBS in studies assessing

219   tumor growth and pharmacodynamics effects can be found in Table 1 and 2, respectively. Tumor

220   volumes were calculated from digital caliper raw data by using the formula: Volume (mm3) =

221   (tumor length x tumor width^2)/2 every two days. During the study, no animal distress or weight

222   lost was observed.

223

224   **Detection of cobomarsen by S1 nuclease protection assay in the xenografts:** Tumor tissue

225   samples were prepared at 100 mg/mL in 3M GITC buffer (3M guanidine-isothiocyanate, 0.5M

226   NaCl, 0.1M Tris, pH 7.5, and 10mM EDTA) by homogenizing with an MP FastPrep-24 tissue

227   homogenizer at a speed setting of 6.0, using two 30-second runs. Tissue homogenates and

228   plasma were diluted in 1M GITC Buffer for testing. Fully complementary 5' biotinylated probes

229   with 3' FITC residues were synthesized and used to capture cobomarsen analyte using 96-well

230   streptavidin coated plates (Roche). Further details are described in the supplementary materials

231   and methods.

232

233   **TUNEL assay:** From the study assessing pharmacodynamic effects (Table 2), tumors were

234   obtained from three mice per group, at 96h post treatment with either PBS alone, 1mg/kg control

235   oligonucleotide or 1mg/kg cobomarsen. Tumor (tissue) slices were embedded in OCT in

236   cryomolds. Cryosections and TUNEL Chromogenic Apoptosis Detection, (kit purchased from

237   Genecopoeia), were performed by the Histology Core of Beth Israel Deaconess Medical Center

238 (Boston, MA). The TUNEL positive area was quantified with ImageJ software. Phase-contrast

239 images were acquired with OLYMPUS BX51 microscope (software DP2-BSW) with 4x and 20x

240 objective. Supplementary information contains further details of the method.

241

242 **Patient selection criteria:** A patient was recruited as part of the clinical trial of safety,

243 tolerability and pharmacokinetics of cobomarsen in patients with MF-CTCL, DLBCL or ATCLL

244 (number NCT02580552), based on the following inclusion criteria: for patients with biopsy-

245 proven DLBCL who are intolerant to, or have disease that is relapsed/refractory after at least two

246 prior therapies, including any anti-CD20 monoclonal antibody and chemotherapy with curative

247 intent. The patient is a 61-year-old female with diabetes, low B12 and peripheral neuropathy who

248 was diagnosed when she presented with left tonsillar enlargement and the biopsy of her tonsillar

249 mass showed DLBCL. The cell of origin of the DLBCL was non-GCB/ABC subtype.

250 The investigators obtained written consent from the patient and the study was performed after

251 approval by institutional review boards of University of California, Irvine, USA. This study was

252 conducted in compliance with the International Conference on Harmonization (ICH) Good

253 Clinical Practice (GCP) Guidelines; United States (US) Code of Federal Regulations (CFR),

254 clinical studies (21 CFR § 50, 56, 312); the Declaration of Helsinki, and with ICH guidelines

255 regarding scientific integrity (E4, E8, E9, and E10).

256

257 **Therapeutic regimens used for the patient:** Prior to cobomarsen clinical trial enrollment, the

258 patient was treated with five regimens, as detailed in Table S1.

259 After the fifth line of treatment, the patient was enrolled in the cobomarsen study, according to

260 the inclusion and exclusion criteria for the clinical trial. The patient was administered 600mg IV

261   infusion of cobomarsen for 5 cycles, each cycle covered 28 days. Physical exams and injections

262   were performed in the same day, as follows: first cycle, six injections at days 1, 3, 5, 12, 19, 26;

263   second, third and fourth cycle, four injections/cycle scheduled at days 1, 8, 15, 22; fifth cycle,

264   three injections at days 1, 8, 15. The nodal tumor mass' longest axis (in cm) measurements were

265   performed at the same indicated days with rulers, since repeated scans of the patient over time

266   were not possible.

267

268   **Statistical analysis:** For the in *vivo* experiments we performed a Power analysis to estimate the

269   group size of NSG mice in order to obtain statistically significant differences between the

270   cobomarsen treated and control groups. All statistical analyses were performed with PRISM7.

271   The statistical significance of the mean value of the tumor volumes in different time points

272   between the groups of mice was performed using 2-way Anova with Sidak's multiple

273   comparisons test.

274   Unpaired, two-tailed t-test analysis was performed for gene expression studies *in vitro,* and for

275   the TUNEL assay.

276

277   **Results**

278

279   **Expression of miR-155 in ABC-DLBCL cell lines**

280   Several studies have shown that miR-155 is generally highly expressed in ABC-DLBCL patients

281   in comparison to healthy controls (29-31). Therefore, we first assessed miR-155 expression in

282   three human ABC-DLBCL cell lines, U2932, OCI-LY3 and RCK8, by qRT-PCR. As expected,

283   all three cell lines expressed high levels of miR-155 (Figure 1A), while the expression of three

284   experimentally validated miR-155 target genes, *HIVEP2, TP53INP1* and *MAFB* (25), was

285   significantly reduced (Figure 1B) compared to CD19+ B cells. Furthermore, we showed that

286   miR-155 expression was higher in the ABC- compared to three GC-DLBCL cell lines

287   (Supplementary Figure S1).

288

289   **Cobomarsen delivery in DLBCL cell lines**

290   To verify functional uptake of the compound, we first transfected cells with a miR-155

291   biosensor, a plasmid which contains a complementary sequence to the mature miR-155 inserted

292   downstream of the *luc* gene. This reporter results in suppression of luciferase expression when

293   the target sequence is bound by endogenous miR-155. Twenty-four hours following transfection

294   of cells with the miR-155 biosensor and after a careful removal of the supernatant, we treated the

295   cell cultures with 10μM of cobomarsen or a control oligonucleotide by adding the compounds

296   directly to the culture medium. Luciferase activity was measured 24h later. Inhibition of

297   endogenous miR-155 by cobomarsen will prevent the binding of miR-155 to the seed-region

298   within the biosensor, which will result in de-repression (increased expression) of the luciferase

299   reporter. As shown in Figure 2A, luciferase activity was significantly de-repressed by

300   cobomarsen in all cell lines compared to the control oligo treatment. These data demonstrate that

301   functional uptake and target engagement by passive delivery of cobomarsen in DLBCL cell lines

302   is efficient even in the presence of higher amounts of miR-155 in the OCI-LY3 and RCK8 cell

303   lines.

304

305   Furthermore, to assess the dose-dependence and sequence specificity on miR-155 activity we

306   treated all three cell lines with three different concentrations of cobomarsen: 2.5 μM, 5 μM and

307   10 μM and subsequently we examined the expression of four previously experimentally

308   validated miR-155 target genes, *BACH1, INPP5D, TP53INP1* and *HIVEP2* (25,32)

309   (Supplementary Figure S2). Our results showed that 10μM cobomarsen treatment of U2932 cell

310   line provided a higher fold change of de-repression of these miR-155 target genes, thus we

311   continued our experiments in U2932 cell line (Supplementary Figure S2A). To estimate the

312   cobomarsen uptake, U2932 cells were treated with 2.5μM and 10μM FITC conjugated

313   compound and analyzed by flow cytometry. As shown in Figure 2B, at 2.5μM and 10μM the

314   FITC MFI (mean fluorescence intensity) was higher compared to the untreated cells, within 6

315   hours, which is indicative that cells have started to take up the compound. Furthermore,

316   internalization of FITC conjugated compound could be obtained even at the lowest

317   concentration, (2.5μM) as seen at 48h post-delivery (Figure 2C). A higher magnification of

318   cobomarsen FITC positive cells clearly enabled us to visualize the compound in the cytoplasm

319   and excluded from the nucleus (Figure 2D). These results show that the compound can be

320   delivered and that it is active inside the cells since it can bind to its target and inhibit it from

321   acting on the complementary sequence of the miR-155 biosensor.

322

323   **Phenotypic impact of Cobomarsen on proliferation and apoptosis in DLBCL cell lines**

324   Several studies have shown that inhibition of miR-155 in lymphoma/leukemia and DLBCL

325   reduces cell proliferation and induces apoptosis (24,33). Therefore, we assessed cell proliferation

326   over time in cobomarsen treated ABC-DLBCL cell lines, in comparison with the control

327   oligonucleotide treated cells. Cells were treated with 10μM cobomarsen for 96h and the

328   luminescence values of metabolically viable cells were estimated at 48h, 72h and 96h (Figure

329   3A). There was a reduction of the luminescence signal, normalized to the control oligonucleotide

330   treated cells, which is directly proportional to the reduction of cellular ATP levels, indicating a

331   decrease in cell proliferation. To examine whether the decrease in proliferation was due to

332   increased apoptosis, all three cell lines were treated with the same amount (10μM) of

333   cobomarsen. Indeed, cobomarsen triggered a significant induction of late apoptosis in all cell

334   lines at 96h post-treatment (Figure 3B). In U2932 and OCI-LY3 cells, treatment with the control

335   oligonucleotide also induced a marginal increase of late apoptotic cells, compared to the

336   untreated cell line. However, the magnitude of effect and the significance of the increased

337   apoptosis were greater with cobomarsen treatment in all cell lines. Collectively, these data

338   demonstrate that inhibition of miR-155 with cobomarsen results in decreased proliferation and

339   increased apoptosis of DLBCL cells.

340

341   **Cobomarsen inhibits tumor growth *in vivo***

342   To determine whether cobomarsen can impact tumor growth *in vivo*, we established xenografts

343   of DLBCL cells expressing high levels of miR-155. While miR-155 expression was elevated in

344   three DLBCL cell lines (Figure 1A), higher expression was observed in OCI-LY3 and RCK8

345   cells. We selected U2932 for xenograft experiments because RCK8 cells did not engraft in mice

346   and OCI-LY3 cells grew too quickly to assess the effect of miR-155 inhibition on tumor growth.

347   Most importantly, we observed that miR-155 target gene de-repression was more pronounced in

348   U2932 cell line treated with cobomarsen, compared with the other two cell lines, (Supplementary

349   figure S2 and S3). Twelve mice each in group A and B, as well as three mice each in group C

350   and D, were i.v. inoculated according to the details described in Table 1 and on days 0, 2, 4 and 7

351   following enrollment into the study, as shown in the experimental timeline (Figure 4A). Tumor

352   volume was measured three days after the last dose or until the tumor volume reached 2000

353   mm^3, until mice were euthanized. Intravenous administration of 1mg/kg cobomarsen reduced

354   tumor growth in group B compared to group A control mice treated with PBS, most significantly

355   at day 7 (**p= 0.0019) and day 10 (****p <0.0001) (Figure 4B). In contrast, there was no impact

356   of the control oligo on tumor volume (group D) in comparison with PBS only treated group C

357   mice (Figure 4C). Both cobomarsen and the control oligonucleotide were well-tolerated and no

358   adverse events were observed.

359

360

361   **Cobomarsen de-represses miR-155 target gene expression *in vivo* and *in vitro***

362   To understand the molecular mechanisms that underlie the reduction of tumor growth by

363   cobomarsen, we assessed whether miR-155 target genes were de-repressed after cobomarsen

364   treatment. The experimental timeline of cobomarsen treated xenografts used to assess

365   pharmacodynamic effects of cobomarsen is shown in figure 5A**.** Mice were inoculated with ten

366   million U2932 cells in the right flank. Mice received two intravenous injections of either PBS

367   alone (vehicle), 1mg/kg cobomarsen or 1mg/kg control oligonucleotide on days 0 and 2

368   following enrollment into the study. Before commencement of the treatment, we ensured that the

369   tumor volume average and standard deviation were similar among the three groups. Tumor tissue

370   was harvested 24 hours after the last dose and either processed to evaluate miR-155 target gene

371   expression or embedded for cryosections to perform the TUNEL assay. The TUNEL assay

372   showed that there are more apoptotic cells (dark brown staining) in the tumor tissues of

373   cobomarsen treated mice, compared to the PBS and control oligonucleotide groups (Figure 5B).

374   Furthermore, the distribution of cobomarsen to all 8 xenografts was successfully detected using a

375   hybridization assay (Figure 5C).

376 A panel of twelve experimentally validated miR-155 target genes, was investigated by qPCR

377 (Figure 5D): *MAFB, SH3PXD2A, SOCS1* (34), *CUX1, WEE1, BACH1, INPP5D, HIVEP2,*

378 *TP53INP1* (25,35), *JARID, PICALM* (26), *CSFR1(36).* Upon cobomarsen treatment, there was a

379 significant de-repression of miR-155 target genes, such as *Cut Like Homeobox 1 (CUX1)*

380 (number 3), *(SH3 And PX Domains 2A) SH3PXD2A, (number 7) Suppressor Of Cytokine*

381 *Signaling 1 (SOCS1)* (number 8) and *WEE1 G2 Checkpoint Kinase (WEE1)* (number 10),

382 between the PBS treated mice comparing to the control oligonucleotide and to the cobomarsen

383 treated group of mice (Figure 5D).

384 Next, we investigated if the de-repression of miR-155 targets observed in cobomarsen treated

385 mice can be recapitulated in three DLBCL cell lines. Two target genes, namely *WEE1* and

386 *CUX1*, were consistently de-repressed in both mice and in cell lines (Figure 5D and 5E). The rest

387 of the genes were variably de-repressed in the two systems (Figure 5D and Supplementary

388 Figure S3). For instance, while *SOCS1* and *SH3PXD2A* were significantly de-repressed in

389 cobomarsen-treated mice, their expression did not change in the three DLBCL cell lines. The

390 expression of *CUX1* was significantly altered in U2932 and OCI-LY3 but not in RCK8 (Figure

391 5E).

392

393 **Cobomarsen as monotherapy**

394 The patient was enrolled immediately (as she had progressive disease) in the clinical trial of

395 cobomarsen (https://clinicaltrials.gov/ct2/show/NCT02580552). The details of patient's prior

396 treatment history and outcome is shown in the Supplementary Material and Methods section. At

397 this time, a radiographic evaluation showed that the patient had developed adenopathy in the

398 right cervical, right parotid, right external iliac and right inguinal areas. On day three of the trial,

399 the patient noted that immediately after the first IV injection (600mg) her right neck mass rapidly

400 increased then decreased in size on the same day. At cycle 1, day three physical examination of

401 her right neck node measured 3.5 cm and her right inguinal node measured 3.0 cm, (Figure 6).

402 By cycle two, day one, the right neck node was no longer palpable, however the right inguinal

403 area was noted to be swollen to 6.0 cm without a definite palpable mass. Two weeks later, on

404 cycle 2, day 15, the right neck remained not palpable and the right inguinal mass had decreased

405 to 2.0 cm. The right inguinal mass continued to decrease until cycle 2, day 27, when there were

406 no palpable nodes found during the physical exam. By cycle 3, day 14, a right supraclavicular

407 node was palpable and measured 1.5 cm. On protocol-mandated computerized tomography (CT)

408 scanning, the patient had progressive disease (PD) because of a new right paratracheal node of

409 1.4 cm, but all other nodes were stable. A right neck fine needle aspiration documented the

410 presence of DLBCL, and at the end of treatment the patient developed her first elevated lactate

411 dehydrogenase (LDH) and increasing lymphadenopathy in the left inguinal and left

412 supraclavicular nodes. The patient was discontinued from the cobomarsen clinical trial after 21

413 total doses of cobomarsen through 5 cycles, as noted in the clinical database (miRagen trial

414 number: MRG106-11-101 and NCT02580552). The reason for discontinuation was documented

415 as early termination due to disease progression, according to the clinical trial criteria.

416 Subsequent to trial participation, the patient had rapidly progressive disease and received one

417 dose of bendamustine in combination with rituximab. The patient then received CAR-T

418 (chimeric antigen receptor T-cell) therapy with an initial radiographic complete response but

419 progressive disease three months after CAR-T infusion. The patient received ibrutinib in

420 combination with rituximab for three months with progressive disease and is currently

421 experiencing a partial response after four doses of polatuzumab in combination with rituximab.

422   She was then treated with polatuzumab achieving a partial response after cycle 4 but progressive

423   disease after cycle 6. The patient has been offered hospice services. As seen by the patient's

424   rapid course after discontinuation of cobomarsen, cobomarsen appeared to reduce the size of

425   sometimes bulky adenopathy demonstrably on physical examination, and stabilize the disease.

426

427   **Discussion**

428   OncomiR-155 expression is highly induced in B-cell lymphoproliferative disorders and in

429   DLBCL, especially in the ABC subtype and it is considered a biomarker for these malignancies

430   (32,37,38). Nevertheless, miRNA-based therapies for cancer treatment are challenging, due to

431   their unfavorable physicochemical properties that may prevent their cellular uptake and

432   distribution in various tissues. Furthermore, miRNA-based therapies may be unstable in plasma

433   and tissues due to the presence of nucleases and endosomal sequestration (18,39,40). To

434   overcome these issues, chemical modifications of RNAs have been incorporated into anti-

435   miRNAs that target oncogenic miRNAs or miRNA mimics that represent tumor suppressive

436   miRNAs to enhance delivery and distribution in the tumor tissue (24) (41) (42). Because of the

437   improvements in delivery approaches and stability of miRNA compounds, clinical trials with

438   such compounds to treat cancer could certainly pave the way for better therapeutic options (43).

439   One of the first promising anti-miR-155 oligonucleotides for therapeutic purpose was an 8-mer

440   locked nucleic acid (LNA) anti-miR-155, delivered systemically in a xenograft mouse model of

441   Waldenstrom macroglobulinemia that decreased tumor growth (34). However, this

442   oligonucleotide has not yet entered into clinical trials. In our study, we assessed cobomarsen, an

443   LNA-based anti-miR-155 compound, in DLBCL, which is now being assessed in a Phase II

444   clinical trial for the treatment of CTCL (https://clinicaltrials.gov/ct2/show/study/NCT03713320).

445 We introduced cobomarsen into human ABC-DLBCL cell lines (with high miR-155 expression),

446 without the assistance of any delivery agent. The anti-miR-155 compound reduced proliferation

447 and induced apoptosis in vitro. In addition, the compound reduced tumor growth of U2932 cell

448 line engraftments in NSG mice. These phenotypic effects were associated with de-repression of

449 miR-155 target genes, both *in vitro* and *in vivo*.

450

451 Very little is known about how miR-155 influences WEE1 and CUX1 in human DLBCL cell

452 lines (34,44). Interestingly, a previous study from our group by Cheng et al., showed that CUX1

453 and WEE1 mRNAs were among miR-155 predicted targets (25). In the same study, it was shown

454 that CUX1 expression is de-repressed after withdrawal of miR-155 in mir-155^{LSLtTA} mice when

455 treated with doxycycline. Our results are consistent with the observations by Cheng et al. CUX1

456 is an evolutionarily conserved transcription factor with two isoforms with diverse functions.

457 Indeed, it acts as a tumor suppressor gene in myeloid neoplasms by regulating cell cycle genes,

458 but its altered expression may also lead to tumor progression (45). Our study demonstrates that

459 there is an induction of cell death upon delivery of cobomarsen *in vitro* and *in vivo*. Further

460 investigation is needed to specifically implicate CUX1 in the reduction of tumor growth.

461

462 WEE1, a G2/M checkpoint tyrosine kinase, catalyzes the inhibitory tyrosine phosphorylation of

463 CDC2/cyclin B kinase. This in turn inhibits mitosis in cells that have damaged genomes and may

464 induce DNA repair or result in cell death (46). Tili et al. have shown that increased expression of

465 miR-155 in breast cancer cell lines induced the proliferation rate by targeting WEE1 transcripts

466 (35). Inhibition of miR-155 with an antisense oligonucleotide in primary B cells of Eµ-miR-155

467 transgenic mice and in breast cancer cell lines released WEE1 expression and caused a block in

468 G2/M transition. In DLBCLs, we find a significant de-repression of WEE1 upon cobomarsen

469 delivery. This is consistent with a tumor suppressive role of the WEE1 gene and confirms the

470 oncogenic nature of miR-155. However, further experiments are needed to conclusively

471 demonstrate the direct tumor suppressive role of WEE1 in DLBCL.

472

473 As mentioned previously, cobomarsen is currently being tested in a first-in-human phase II

474 clinical trial in patients with MF-CTCL, https://clinicaltrials.gov/ct2/show/study/NCT03713320.

475 In addition, a study showed that cobomarsen had anti-proliferative, pro-apoptotic effects in MF

476 and human lymphotropic virus type 1 (HTLV-1+) CTCL cell lines *in vitro* (26). Another phase I

477 clinical   trial   (https://clinicaltrials.gov/ct2/show/NCT02580552)   is   currently   evaluating

478 cobomarsen-treated ATLL, CLL patients. We have begun to assess the safety and therapeutic

479 utility of cobomarsen, particularly for a relapsing case of ABC-DLBCL. A patient affected by

480 ABC-DLBCL previously treated with chemotherapeutic regimens but relapsing, was enrolled for

481 cobomarsen treatment. In contrast with other therapeutic strategies, cobomarsen treatment

482 resulted in a significant decrease of tumor nodes with apparently no side-effects. To our

483 knowledge, this is the first miRNA-based therapy that had beneficial outcome for the patient

484 with no toxicity. This level of disease stabilization with minimal toxicity is uncommon for an

485 investigational agent in the face of a very aggressive B-cell lymphoma. Clearly, these findings

486 need to be confirmed in more patients in the future clinical trial to better evaluate

487 pharmacodynamics and safety of cobomarsen therapy against hard-to treat lymphomas.

488

489 Several reports suggest that miR-155 is deregulated in virus infected lymphomas like Burkitt

490 lymphoma (BL). It is known that Epstein-Barr virus (EBV) alters cellular miRNA expression in

491   B lymphomas (47) (48) (49) (50) (51) (52). Other viruses like HHV-8 and Marek's disease virus

492   (MDV) have a viral miRNA homologue of miR-155 with identical seed sequence (53). This

493   suggests that deregulation of either cellular miR-155 or its viral miRNA orthologues is important

494   for virus associated lymphomas (54). Our study could extend the therapeutic potential of

495   cobomarsen for such lymphomas as well.

496

497   In conclusion, more effective therapies are urgently needed to cure refractory or relapsed

498   DLBCL. Our preclinical studies support the use of cobomarsen for the treatment of patients with

499   DLBCL with high miR-155, for the therapeutic management of DLBCL patients. The results

500   observed in one only patient here, might provide impetus for the continuation and extension of

501   cobomarsen-based therapy not only for ABC-DLBCLs but other lymphomas with high miR-155

502   expression.

503

504

505

506

507

508

513

514 **Author contributions**

515 E.A., F.J.S., A.L.J., A.G.S. designed the research studies. E.A. performed the research *in vitro*

516 and *in vivo.* E.G. analyzed TUNEL assay data. D.S. and E.A. performed flow cytometry analysis.

517 E.A., A.G.S., M.H. and X.B., analyzed the gene expression data, L.C. P.B. was the patient's

518 treating physician and wrote the patient's case report. E.A. wrote the first draft. All authors have

519 critically revised each draft of the manuscript and approved the final version of the manuscript.

520

521

522

523

524 **References**

525

526 1.   Alizadeh AA, Eisen MB, Davis RE, Ma C, Lossos IS, Rosenwald A*, et al.* Distinct types

527   of diffuse large B-cell lymphoma identified by gene expression profiling. Nature

528   **2000**;403(6769):503-11 doi 10.1038/35000501.

529 2.   Li S, Young KH, Medeiros LJ. Diffuse large B-cell lymphoma. Pathology **2018**;50(1):74-

530   87 doi 10.1016/j.pathol.2017.09.006.

531 3.   Sehn LH, Berry B, Chhanabhai M, Fitzgerald C, Gill K, Hoskins P*, et al.* The revised

532   International Prognostic Index (R-IPI) is a better predictor of outcome than the standard

533   IPI for patients with diffuse large B-cell lymphoma treated with R-CHOP. Blood

534   **2007**;109(5):1857-61 doi 10.1182/blood-2006-08-038257.

535   4.   Nowakowski GS, Czuczman MS. ABC, GCB, and Double-Hit Diffuse Large B-Cell

536   Lymphoma: Does Subtype Make a Difference in Therapy Selection? Am Soc Clin Oncol

537   Educ Book **2015**:e449-57 doi 10.14694/EdBook_AM.2015.35.e449.

538   5.   Chapuy B, Stewart C, Dunford AJ, Kim J, Kamburov A, Redd RA*, et al.* Molecular

539   subtypes of diffuse large B cell lymphoma are associated with distinct pathogenic

540   mechanisms and outcomes. Nat Med **2018**;24(5):679-90 doi 10.1038/s41591-018-0016-8.

541   6.   Schmitz R, Wright GW, Huang DW, Johnson CA, Phelan JD, Wang JQ*, et al.* Genetics

542   and Pathogenesis of Diffuse Large B-Cell Lymphoma. N Engl J Med **2018**;378(15):1396-

543   407 doi 10.1056/NEJMoa1801445.

544   7.   Horn H, Ziepert M, Becher C, Barth TF, Bernd HW, Feller AC*, et al.* MYC status in

545   concert with BCL2 and BCL6 expression predicts outcome in diffuse large B-cell

546   lymphoma. Blood **2013**;121(12):2253-63 doi 10.1182/blood-2012-06-435842.

547   8.   Visco C, Tzankov A, Xu-Monette ZY, Miranda RN, Tai YC, Li Y*, et al.* Patients with

548   diffuse large B-cell lymphoma of germinal center origin with BCL2 translocations have

549   poor outcome, irrespective of MYC status: a report from an International DLBCL

550   rituximab-CHOP Consortium Program Study. Haematologica **2013**;98(2):255-63 doi

551   10.3324/haematol.2012.066209.

552   9.   Tilly H, Gomes da Silva M, Vitolo U, Jack A, Meignan M, Lopez-Guillermo A*, et al.*

553   Diffuse large B-cell lymphoma (DLBCL): ESMO Clinical Practice Guidelines for

554   diagnosis, treatment and follow-up. Ann Oncol **2015**;26 Suppl 5:v116-25 doi

555   10.1093/annonc/mdv304.

556   10.   Younes A, Thieblemont C, Morschhauser F, Flinn I, Friedberg JW, Amorim S*, et al.*

557   Combination of ibrutinib with rituximab, cyclophosphamide, doxorubicin, vincristine,

558   and prednisone (R-CHOP) for treatment-naive patients with CD20-positive B-cell non-

559   Hodgkin lymphoma: a non-randomised, phase 1b study. Lancet Oncol **2014**;15(9):1019-

560   26 doi 10.1016/s1470-2045(14)70311-0.

561 11. Nowakowski GS, LaPlant B, Macon WR, Reeder CB, Foran JM, Nelson GD*, et al.*

562   Lenalidomide combined with R-CHOP overcomes negative prognostic impact of non-

563   germinal center B-cell phenotype in newly diagnosed diffuse large B-Cell lymphoma: a

564   phase II study. J Clin Oncol **2015**;33(3):251-7 doi 10.1200/jco.2014.55.5714.

565 12. Vaidya R, Witzig TE. Prognostic factors for diffuse large B-cell lymphoma in the

566   R(X)CHOP era. Ann Oncol **2014**;25(11):2124-33 doi 10.1093/annonc/mdu109.

567 13. Coiffier B, Sarkozy C. Diffuse large B-cell lymphoma: R-CHOP failure-what to do?

568   Hematology Am Soc Hematol Educ Program **2016**;2016(1):366-78 doi

569   10.1182/asheducation-2016.1.366.

570 14. Anastasiadou E, Jacob LS, Slack FJ. Non-coding RNA networks in cancer. Nat Rev

571   Cancer **2018**;18(1):5-18 doi 10.1038/nrc.2017.99.

572 15. Higgs G, Slack F. The multiple roles of microRNA-155 in oncogenesis. J Clin

573   Bioinforma **2013**;3(1):17 doi 10.1186/2043-9113-3-17.

574 16. Di Marco M, Ramassone A, Pagotto S, Anastasiadou E, Veronese A, Visone R.

575   MicroRNAs in Autoimmunity and Hematological Malignancies. Int J Mol Sci

576   **2018**;19(10) doi 10.3390/ijms19103139.

577 17. Lawrie CH, Gal S, Dunlop HM, Pushkaran B, Liggins AP, Pulford K*, et al.* Detection of

578   elevated levels of tumour-associated microRNAs in serum of patients with diffuse large

579   B-cell lymphoma. Br J Haematol **2008**;141(5):672-5 doi 10.1111/j.1365-

580   2141.2008.07077.x.

581   18.   Due H, Svendsen P, Bodker JS, Schmitz A, Bogsted M, Johnsen HE*, et al.* miR-155 as a

582   Biomarker in B-Cell Malignancies. Biomed Res Int **2016**;2016:9513037 doi

583   10.1155/2016/9513037.

584   19.   Sole C, Arnaiz E, Lawrie CH. MicroRNAs as Biomarkers of B-cell Lymphoma. Biomark

585   Insights **2018**;13:1177271918806840 doi 10.1177/1177271918806840.

586   20.   Tam W. Identification and characterization of human BIC, a gene on chromosome 21 that

587   encodes a noncoding RNA. Gene **2001**;274(1-2):157-67 doi 10.1016/s0378-

588   1119(01)00612-6.

589   21.   Lawrie CH, Soneji S, Marafioti T, Cooper CD, Palazzo S, Paterson JC*, et al.* MicroRNA

590   expression distinguishes between germinal center B cell-like and activated B cell-like

591   subtypes of diffuse large B cell lymphoma. Int J Cancer **2007**;121(5):1156-61 doi

592   10.1002/ijc.22800.

593   22.   Eis PS, Tam W, Sun L, Chadburn A, Li Z, Gomez MF*, et al.* Accumulation of miR-155

594   and BIC RNA in human B cell lymphomas. Proc Natl Acad Sci U S A

595   **2005**;102(10):3627-32 doi 10.1073/pnas.0500613102.

596   23.   Costinean S, Zanesi N, Pekarsky Y, Tili E, Volinia S, Heerema N*, et al.* Pre-B cell

597   proliferation and lymphoblastic leukemia/high-grade lymphoma in E(mu)-miR155

598   transgenic mice. Proc Natl Acad Sci U S A **2006**;103(18):7024-9 doi

599   10.1073/pnas.0602266103.

600   24.   Babar IA, Cheng CJ, Booth CJ, Liang X, Weidhaas JB, Saltzman WM*, et al.*

601   Nanoparticle-based therapy in an in vivo microRNA-155 (miR-155)-dependent mouse

602   model of lymphoma. Proc Natl Acad Sci U S A **2012**;109(26):E1695-704 doi

603   10.1073/pnas.1201516109.

604   25.   Cheng CJ, Bahal R, Babar IA, Pincus Z, Barrera F, Liu C, *et al.* MicroRNA silencing for

605   cancer therapy targeted to the tumour microenvironment. Nature **2015**;518(7537):107-10

606   doi 10.1038/nature13905.

607   26.   Seto AG, Beatty X, Lynch JM, Hermreck M, Tetzlaff M, Duvic M, *et al.* Cobomarsen, an

608   oligonucleotide inhibitor of miR-155, co-ordinately regulates multiple survival pathways

609   to reduce cellular proliferation and survival in cutaneous T-cell lymphoma. Br J

610   Haematol **2018**;183(3):428-44 doi 10.1111/bjh.15547.

611   27.   Ramachandiran S, Adon A, Guo X, Wang Y, Wang H, Chen Z, *et al.* Chromosome

612   instability in diffuse large B cell lymphomas is suppressed by activation of the

613   noncanonical NF-kappaB pathway. Int J Cancer **2015**;136(10):2341-51 doi

614   10.1002/ijc.29301.

615   28.   Cirone M, Conte V, Farina A, Valia S, Trivedi P, Granato M, *et al.* HHV-8 reduces

616   dendritic cell migration through down-regulation of cell-surface CCR6 and CCR7 and

617   cytoskeleton reorganization. Virol J **2012**;9:92 doi 10.1186/1743-422x-9-92.

618   29.   Huskova H, Korecka K, Karban J, Vargova J, Vargova K, Dusilkova N, *et al.* Oncogenic

619   microRNA-155 and its target PU.1: an integrative gene expression study in six of the

620   most prevalent lymphomas. Int J Hematol **2015**;102(4):441-50 doi 10.1007/s12185-015-

621   1847-4.

622   30.   Lim EL, Trinh DL, Scott DW, Chu A, Krzywinski M, Zhao Y, *et al.* Comprehensive

623   miRNA sequence analysis reveals survival differences in diffuse large B-cell lymphoma

624   patients. Genome Biol **2015**;16:18 doi 10.1186/s13059-014-0568-y.

625   31.   Musilova K, Mraz M. MicroRNAs in B-cell lymphomas: how a complex biology gets

626   more complex. Leukemia **2015**;29(5):1004-17 doi 10.1038/leu.2014.351.

627   32.   Mazan-Mamczarz K, Gartenhaus RB. Role of microRNA deregulation in the

628   pathogenesis of diffuse large B-cell lymphoma (DLBCL). Leuk Res **2013**;37(11):1420-8

629   doi 10.1016/j.leukres.2013.08.020.

630   33.   Zhu FQ, Zeng L, Tang N, Tang YP, Zhou BP, Li FF, *et al.* MicroRNA-155

631   Downregulation Promotes Cell Cycle Arrest and Apoptosis in Diffuse Large B-Cell

632   Lymphoma. Oncol Res **2016**;24(6):415-27 doi 10.3727/096504016x14685034103473.

633   34.   Zhang Y, Roccaro AM, Rombaoa C, Flores L, Obad S, Fernandes SM, *et al.* LNA-

634   mediated anti-miR-155 silencing in low-grade B-cell lymphomas. Blood

635   **2012**;120(8):1678-86 doi 10.1182/blood-2012-02-410647.

636   35.   Tili E, Michaille JJ, Wernicke D, Alder H, Costinean S, Volinia S, *et al.* Mutator activity

637   induced by microRNA-155 (miR-155) links inflammation and cancer. Proc Natl Acad Sci

638   U S A **2011**;108(12):4908-13 doi 10.1073/pnas.1101795108.

639   36.   Riepsaame J, van Oudenaren A, den Broeder BJ, van Ijcken WF, Pothof J, Leenen PJ.

640   MicroRNA-Mediated Down-Regulation of M-CSF Receptor Contributes to Maturation of

641   Mouse Monocyte-Derived Dendritic Cells. Front Immunol **2013**;4:353 doi

642   10.3389/fimmu.2013.00353.

643   37.   Caramuta S, Lee L, Ozata DM, Akcakaya P, Georgii-Hemming P, Xie H, *et al.* Role of

644   microRNAs and microRNA machinery in the pathogenesis of diffuse large B-cell

645   lymphoma. Blood Cancer J **2013**;3:e152 doi 10.1038/bcj.2013.49.

646   38.   Lim EL, Trinh DL, Scott DW, Chu A, Krzywinski M, Zhao Y, *et al.* Comprehensive

647   miRNA sequence analysis reveals survival differences in diffuse large B-cell lymphoma

648   patients. Genome biology **2015**;16(1):18- doi 10.1186/s13059-014-0568-y.

649   39.   Kaczmarek JC, Kowalski PS, Anderson DG. Advances in the delivery of RNA

650   therapeutics: from concept to clinical reality. Genome Med **2017**;9(1):60 doi

651   10.1186/s13073-017-0450-0.

652   40.   Yin W, Rogge M. Targeting RNA: A Transformative Therapeutic Strategy. Clin Transl

653   Sci **2019**;12(2):98-112 doi 10.1111/cts.12624.

654   41.   Gilles ME, Hao L, Huang L, Rupaimoole R, Lopez-Casas PP, Pulver E*, et al.*

655   Personalized RNA Medicine for Pancreatic Cancer. Clin Cancer Res **2018**;24(7):1734-47

656   doi 10.1158/1078-0432.Ccr-17-2733.

657   42.   Malik S, Bahal R. Investigation of PLGA nanoparticles in conjunction with nuclear

658   localization sequence for enhanced delivery of antimiR phosphorothioates in cancer cells

659   in vitro. J Nanobiotechnology **2019**;17(1):57 doi 10.1186/s12951-019-0490-2.

660   43.   Rupaimoole R, Slack FJ. MicroRNA therapeutics: towards a new era for the management

661   of cancer and other diseases. Nat Rev Drug Discov **2017**;16(3):203-22 doi

662   10.1038/nrd.2016.246.

663   44.   Jiang S, Zhang HW, Lu MH, He XH, Li Y, Gu H*, et al.* MicroRNA-155 functions as an

664   OncomiR in breast cancer by targeting the suppressor of cytokine signaling 1 gene.

665   Cancer Res **2010**;70(8):3119-27 doi 10.1158/0008-5472.Can-09-4250.

666   45.   Ramdzan ZM, Nepveu A. CUX1, a haploinsufficient tumour suppressor gene

667   overexpressed in advanced cancers. Nat Rev Cancer **2014**;14(10):673-82 doi

668   10.1038/nrc3805.

669   46.   Matheson CJ, Backos DS, Reigan P. Targeting WEE1 Kinase in Cancer. Trends

670   Pharmacol Sci **2016**;37(10):872-81 doi 10.1016/j.tips.2016.06.006.

671   47.   Anastasiadou E, Boccellato F, Vincenti S, Rosato P, Bozzoni I, Frati L*, et al.* Epstein-

672   Barr virus encoded LMP1 downregulates TCL1 oncogene through miR-29b. Oncogene

673   **2010**;29(9):1316-28 doi 10.1038/onc.2009.439.

674   48.   Anastasiadou E, Garg N, Bigi R, Yadav S, Campese AF, Lapenta C*, et al.* Epstein-Barr

675   virus infection induces miR-21 in terminally differentiated malignant B cells. Int J

676   Cancer **2015**;137(6):1491-7 doi 10.1002/ijc.29489.

677   49.   Anastasiadou E, Stroopinsky D, Alimperti S, Jiao AL, Pyzer AR, Cippitelli C*, et al.*

678   Epstein-Barr virus-encoded EBNA2 alters immune checkpoint PD-L1 expression by

679   downregulating miR-34a in B-cell lymphomas. Leukemia **2019**;33(1):132-47 doi

680   10.1038/s41375-018-0178-x.

681   50.   Di Napoli A, Al-Jadiri MF, Talerico C, Duranti E, Pilozzi E, Trivedi P*, et al.* Epstein-

682   Barr virus (EBV) positive classical Hodgkin lymphoma of Iraqi children: an

683   immunophenotypic and molecular characterization of Hodgkin/Reed-Sternberg cells.

684   Pediatr Blood Cancer **2013**;60(12):2068-72 doi 10.1002/pbc.24654.

685   51.   Rosato P, Anastasiadou E, Garg N, Lenze D, Boccellato F, Vincenti S*, et al.* Differential

686   regulation of miR-21 and miR-146a by Epstein-Barr virus-encoded EBNA2. Leukemia

687   **2012**;26(11):2343-52 doi 10.1038/leu.2012.108.

688   52.   Trivedi P, Slack FJ, Anastasiadou E. Epstein-Barr virus: From kisses to cancer, an

689   ingenious immune evader. Oncotarget **2018**;9(92):36411-2 doi

690   10.18632/oncotarget.26381.

691   53.   Gottwein E, Mukherjee N, Sachse C, Frenzel C, Majoros WH, Chi JT*, et al.* A viral

692   microRNA functions as an orthologue of cellular miR-155. Nature **2007**;450(7172):1096-

693   9 doi 10.1038/nature05992.

694 54. Zhao Y, Xu H, Yao Y, Smith LP, Kgosana L, Green J, *et al.* Critical role of the virus-

695   encoded microRNA-155 ortholog in the induction of Marek's disease lymphomas. PLoS

696   Pathog **2011**;7(2):e1001305 doi 10.1371/journal.ppat.1001305.

697

698

699

700

701

702 **Table 1:** Tumor xenograft growth study

Group[a]	Number of mice/group	Dose	Miragen compounds	Route of administration	Schedule[b]
A	12	100μl	PBS	i.v.	day 0, 2, 4 and 7 following enrollment into group
B	12	1 mg/kg	Cobomarsen	i.v.	day 0, 2, 4 and 7 following enrollment into group
C	3	100μl	PBS	i.v.	day 0, 2, 4 and 7 following enrollment into group
D	3	1 mg/kg	Control oligonucleotide	i.v.	day 0, 2, 4 and 7 following enrollment into group

703 [a] Five-to-six week old female NSG (*NOD*.Cg-Prkdc^{scid} Il2rg^{tm1Wjl}/SzJ, strain n. 005557) mice

704 were divided in four groups: A and B contained 12 mice each that were injected intravenously

705 (i.v.), in the tail vein, with 100μl of the vehicle PBS (phosphate buffered saline) or with 1mg/kg

706   cobomarsen, respectively. Group A served as control for group B. The C and D groups contained

707   3 mice each, injected i.v. either with 100μl PBS alone or 100μl PBS containing 1mg/kg of the

708   control oligonucleotide, respectively. Group C served as control for group D. [b]For the tumor

709   growth study the time points of i.v. injections were scheduled as described in the table.

710
711

712

713

714   **Table 2:** Pharmacodynamic study

Group[a]	Number of mice/group	Dose	Miragen compounds	Route of administration	Schedule[b]
1	8	100μl	PBS	i.v.	Injection at 0 and 48 hours post enrollment
2	8	1 mg/kg	control oligonucleotide	i.v.	Injection at 0 and 48 hours post enrollment
3	8	1 mg/kg	cobomarsen	i.v.	Injection at 0 and 48 hours post enrollment

715   [a] Five-to-six-week-old female NSG (*NOD*.Cg-Prkdc^{scid} Il2rg^{tm1Wjl}/SzJ, strain n. 005557) mice

716   were divided in three groups: 1, 2 and 3 containing 8 mice each. All mice were injected

717   intravenously (i.v.) in the tail vein, with 100μl of the vehicle PBS, the second with 100 μl of

718   1mg/kg control oligonucleotide in PBS and the third with 100 μl of 1mg/kg of Cobomarsen in

719   PBS.

720   [b] For the pharmacodynamic study all the injections were performed at the beginning of the study,

721   indicated as 0 and at 48 hours post enrollment.

722
723

724

725

726

727

728

729

730

731

732 **Figure legends**

733 **Figure 1: High expression of miR-155 in DLBCL cell lines and correlation with target gene**

734 **expression**

735 **A. The fold change of miR-155 expression in three ABC-type DLBCL cell lines was**

736 **assessed by qRT-PCR.** MiR-155 fold change was compared to CD19 B+ isolated from healthy

737 donors and normalized to RNU6 housekeeping gene. Statistical analysis was performed with

738 unpaired, two tailed t test ****$p<0.0001$. Fold change represent the average ($\pm$ standard

739 deviation, SD) of three independent experiments, each performed in technical triplicates.

740 **B. The fold change of miR-155 target genes, HIVEP2, TP53INP1 and MAFB expression**

741 **was assessed by qRT-PCR:** The fold change expression of each target gene in each cell line

742 was compared to the one of CD19 B+ cells and was normalized to GAPDH. Unpaired, two tailed

743 t test was applied: ****$p<0.0001$. Fold change represent the average ($\pm$ standard deviation, SD)

744 of three independent experiments, each performed in technical triplicates.

745

746   **Figure 2: Unassisted delivery of cobomarsen in ABC-DLBCL cell lines**

747   **A. Reduction in endogenous miR-155 activity by cobomarsen:** Luciferase activity was

748   measured 24 hours after treatment with Cobomarsen or control oligonucleotide. Each treatment

749   was performed in triplicates and the experiment was repeated three times. Relative luminescence

750   units (RLU) indicate the ratio of Renilla luciferase (hRluc) expression normalized against firefly

751   luciferase (fluc), (hRluc/fluc), of the miR-155 biosensor. The control oligo and Cobomarsen

752   treated cell lines were compared. Unpaired, two tailed t test was applied as a mean value for each

753   experiment repeated three times and in triplicates. The calculated p values between control oligo

754   treated versus cobomarsen treated cell line are: U2932:$**p<0.01$, OCI-LY3:$****p<0.0001$,

755   RCK8:$***p<0.001$.

756   **B. cobomarsen uptake in recipient lymphoma cells:** Two different concentrations (2.5μM,

757   10μM) of FITC conjugated cobomarsen were directly added in the culture of U2932 cell line.

758   Histograms show the mean fluorescence intensity (MFI) at both concentrations comparing to the

759   cobomarsen untreated cells, at six hours post-delivery. MFI was measured by flow cytometer and

760   the data were analyzed by Kaluza for Gallios Software.

761   **C and D. Subcellular localization of cobomarsen: C.** Confocal microscopy images of 2.5μM

762   FITCH conjugated cobomarsen in U2932 cell line at 48h post-delivery. **D.** A higher

763   magnification (20x) demonstrates cobomarsen as green fluorescent dot next to the nucleus, blue

764   colored, with 4′,6-diamidino-2-phenylindole (DAPI). Confocal images were acquired using 20x

765   and 10x objectives with the Zeiss LSM 880 confocal microscope.

766

767   **Figure 3: Proliferation and apoptosis in DLBCL cell lines upon cobomarsen treatment**

768　**A.** The proliferation graphs indicate luminescence (RLU) measurements as a ratio of

769　cobomarsen/control oligonucleotide RLU at 48h, 72h and 96h post-delivery of 10μM

770　cobomarsen or 10μM control oligonucleotide. The experiment was performed three times and in

771　triplicates. Unpaired, two tailed t test was applied to calculate the statistical significance of the

772　difference between the average of RLU ratio measurements at 72h and 96 h compared to

773　corresponding average of RLU at 48h . *$p<0.05$, **$p<0.01$.

774　**B.** Annexin V/PI measurement of late apoptotic cells (double stained for Annexin V and PI) 96

775　hours following treatment with 10μM cobomarsen. For each cell line the % of late apoptotic

776　cells, upon treatment was compared with the % of untreated cells, by setting the same threshold.

777　One out of three representative experiments is shown. The histograms for each cell line, at the

778　right side of the figure, show the mean values from three independent apoptosis assays,

779　comparing the % of untreated, control oligonucleotide and cobomarsen treated cells. U2932,

780　*$p<0.05$, **$p<0.01$, ****$p<0.0001$. OCY-LY3, *$p<0.05$, **$p<0.01$, ***$p<0.001$. RCK8,

781　**$p<0.01$, ***$p<0.001$. Statistical analysis was performed with unpaired, two tailed t test.

782　Kaluza for Gallios Software was used for analysis.

783

784　**Figure 4: Effect of cobomarsen on tumor growth *in vivo***

785　**A. Timeline of in vivo inoculations of cobomarsen and control oligonucleotide:** The tumors

786　began to grow 9-12 days after injection. Mice were enrolled in the study when the tumor volume

787　reached a range of 150-200mm^3. Subsequently, 12 mice were injected intravenously with 100μl

788　PBS and 12mice with 1mg/kg cobomarsen. In parallel, 3 mice were injected with 100μl PBS and

789　3 mice with 1mg/kg of a control oligonucleotide on days 0, 2, 4 and 7 post-enrollment. 72 hours

790   after the last dose, mice were euthanized. All tumor volume measurements were taken before the

791   injections.

792   **B. Tumor growth:** The mean value of the calculated volumes (mm^3) of the xenografts at the

793   indicated time points, in 12 mice treated with 1mg/kg cobomarsen in comparison with the mean

794   of the calculated volumes in 12 mice treated with 100μl PBS, show a significant reduction in

795   time, at the 7th day and at the 10th day, of 12 mice **p<0.01, ****p <0.0001

796   **C. Tumor growth:** The mean value of the calculated volumes (mm^3) of the xenografts and in the

797   indicated time points show no difference between the groups of 3 mice treated with 100μl PBS

798   comparing with the group of 3 mice treated with 1mg/ml control oligo.

799   The statistical significance of the mean value of the tumor volumes in different time points

800   between the groups of mice was performed using 2-way Anova with Sidak's multiple

801   comparisons test.

802

803   **Figure 5: cobomarsen de-represses miR-155 target gene expression *in vivo* and *in vitro***

804   **A. Timeline of cobomarsen treated xenografts used to assess pharmacodynamic effects:**

805   Mice were randomly enrolled into groups when tumors reached a volume of 150-200mm^3 (N=8

806   for each of 3 groups; PBS, control oligonucleotide and cobomarsen). Mice were injected

807   intravenously with either PBS, 1mg/kg control oligonucleotide or 1mg/kg cobomarsen at 0 and

808   48 hours post-enrollment. 24 hours after the last dose, mice were sacrificed and tumor tissue was

809   harvested.

810   **B. cobomarsen induces tumor apoptosis:** Detection of apoptotic cells in mice tumor tissues

811   24 hours following the final dose of PBS, control oligonucleotide or cobomarsen. Three

812   representative photos of mouse tumor tissue cryosections processed with the TUNEL

813   chromogenic apoptotic assay. Chromogen 3,3′-Diaminobenzidine (DAB) staining reveals the

814   brown spots which indicate apoptotic cells. The analysis was performed for a total of 4-10 fields

815   per tumor. The results are reported as Arbitrary Unit (AU) and represent an average value from 3

816   mice per treatment (PBS, 1 mg/kg-control oligonucleotide, 1mg/kg cobomarsen). Statistical

817   analysis was performed with unpaired, two tailed t test. **$p < 0.01$ for cobomarsen vs. PBS, and

818   for cobomarsen vs. control oligo.

819   **C. Drug distribution in tumor tissue**: Quantification of cobomarsen in the tumors from treated

820   mice (n=8), represented by black dots, using S1 nuclease protection assay.

821   **D. qRT-PCR analysis of miR-155 target gene expression in cobomarsen treated xenografts:**

822   Mice were euthanized, and tumors were harvested 24 hours after the last injection with either

823   PBS, control oligonucleotide or cobomarsen. RNA was extracted from tumors and the expression

824   of direct miR-155 target genes was evaluated by qRT-PCR. Two-way ANOVA, Tukey's

825   multiple comparison test, between the mean values of miR-155 target gene expression per

826   treatment from group of mice treated with PBS versus oligonucleotide control

827   treated,****$p < 0.0001$ and between the group of mice treated with oligonucleotide versus

828   cobomarsen treated ***$p < 0.001$. N=8 mice per group.

829   **E. miR-155 target genes are de-repressed in cobomarsen treated DLBCL cell lines**: qRT-

830   PCR analysis of miR-155 target genes, CUX1 and WEE1 upon treatment with 10μM

831   cobomarsen, at 96h in U2932, OCI-LY3 and RCK8 DLBCLs. (for U2932 CUX1: ****$p < 0.0001$

832   and WEE1 ***$p < 0.001$, **$p < 0.01$. For OCI-LY3 CUX1: ***$p < 0.001$ and WEE1: **$p < 0.01$. For

833   RCK8 CUX1, n.s.: $p = 0.1851$ and WEE1: *$p < 0.05$. P values were calculated with unpaired, two

834   tailed t test. The experiment was performed in triplicates and repeated at least two times.

835

836 **Figure 6: Patient's lymph node (LN) measurements over time, during the cobomarsen**

837 **treatment.**

838 The longest axis of right (R) cervical lymph nodes (LN), R inguinal LN and left (L) inguinal LN

839 was measured with a ruler after palpable medical examinations of the tumor mass. The size of

840 the tumor mass in cm was assessed at the indicated days for each of the 5 cycles. Cobomarsen IV

841 injections (600mg/injection) were performed at the same day as the physical exams and

842 measurements (1st cycle: 6 injections. 2nd, 3rd, and 4th cycle: 4 injections/cycle and 5th cycle: 3

843 injections). LN measurements were performed during physical examination, at the days indicated

844 in the graph: for R Cervical LN the measurements were started at cycle 1, day 1, while for R

845 inguinal LN measurements were started at cycle 1, day 3. L inguinal LN was noted during the

846 cycle 3 on the 22th day.
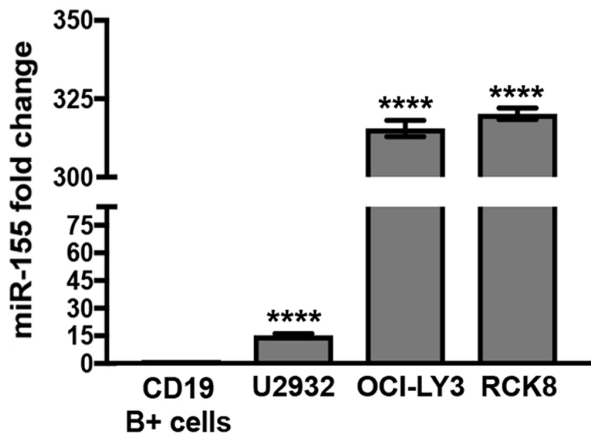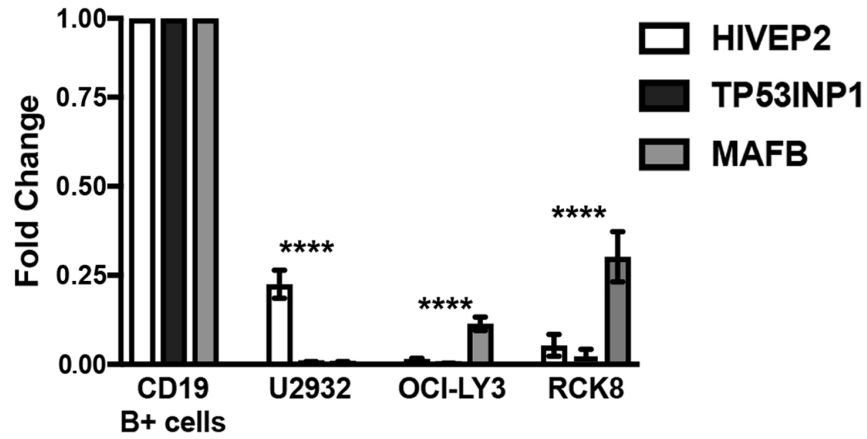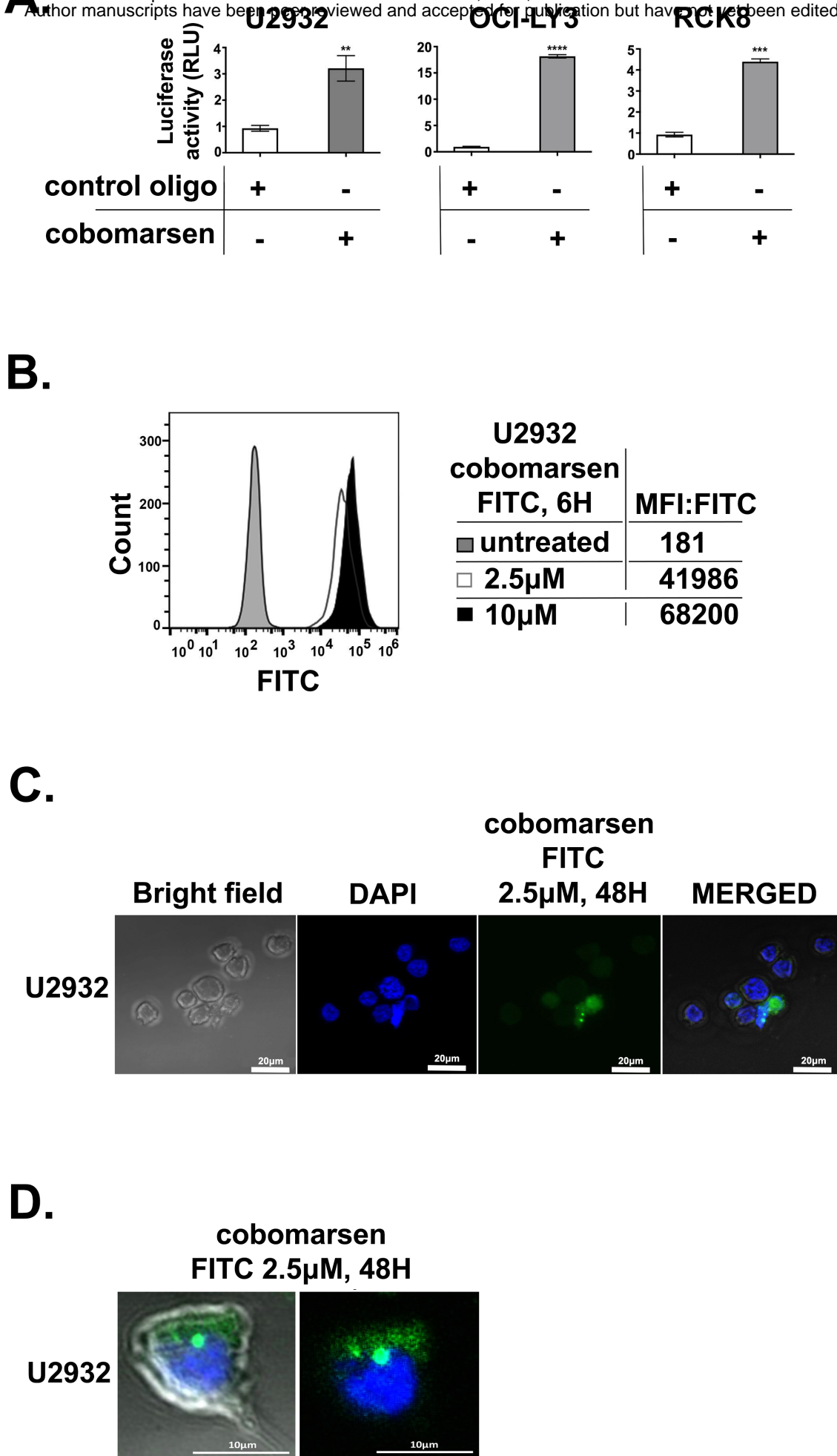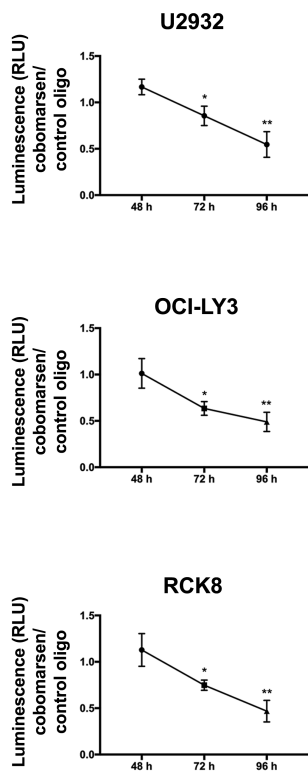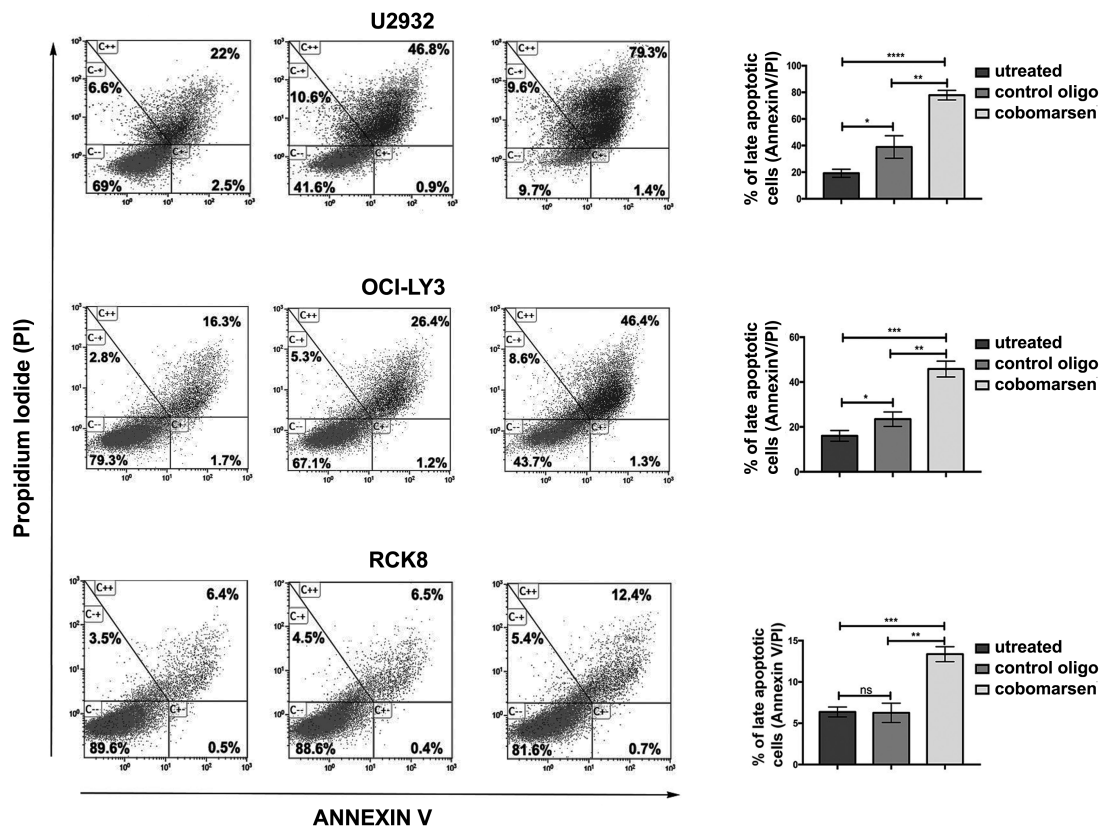
Figure 1
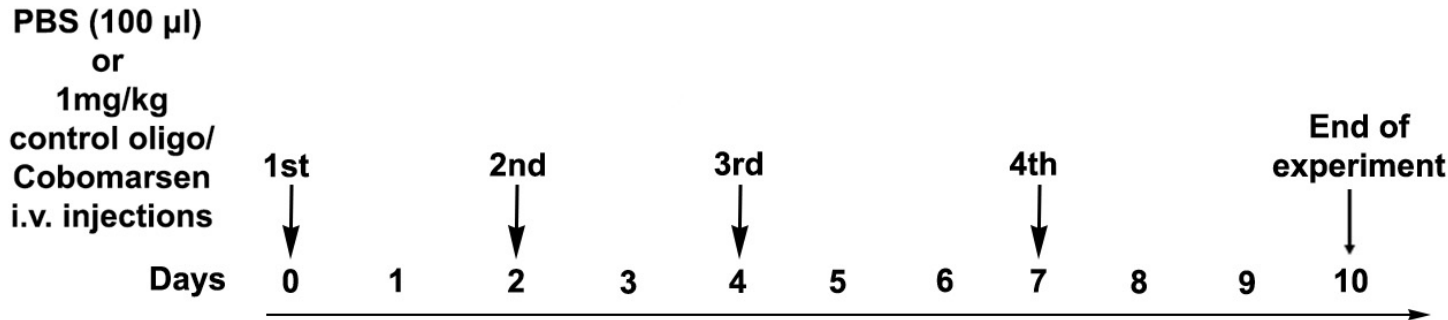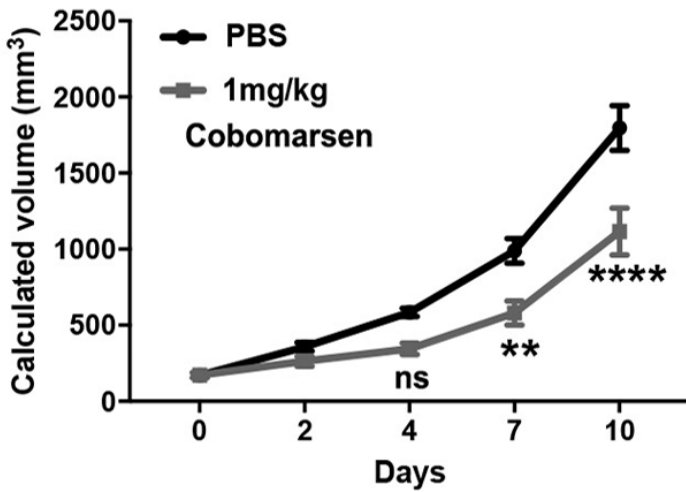
Figure 2

Figure 3

Figure 4

Figure 5

Figure 6

AAGR American Association for Cancer Research
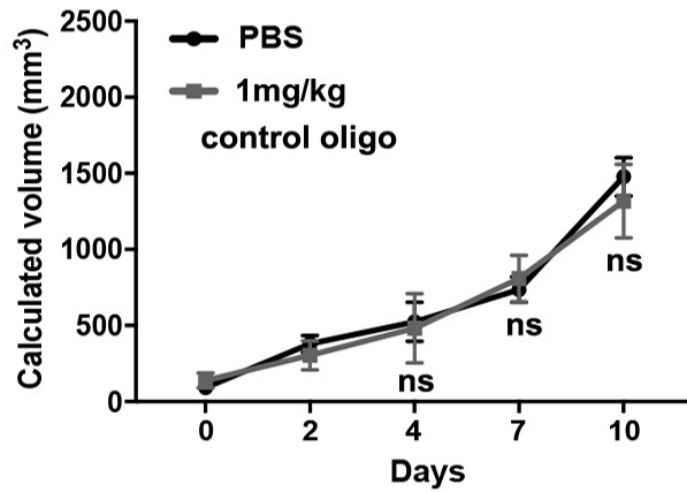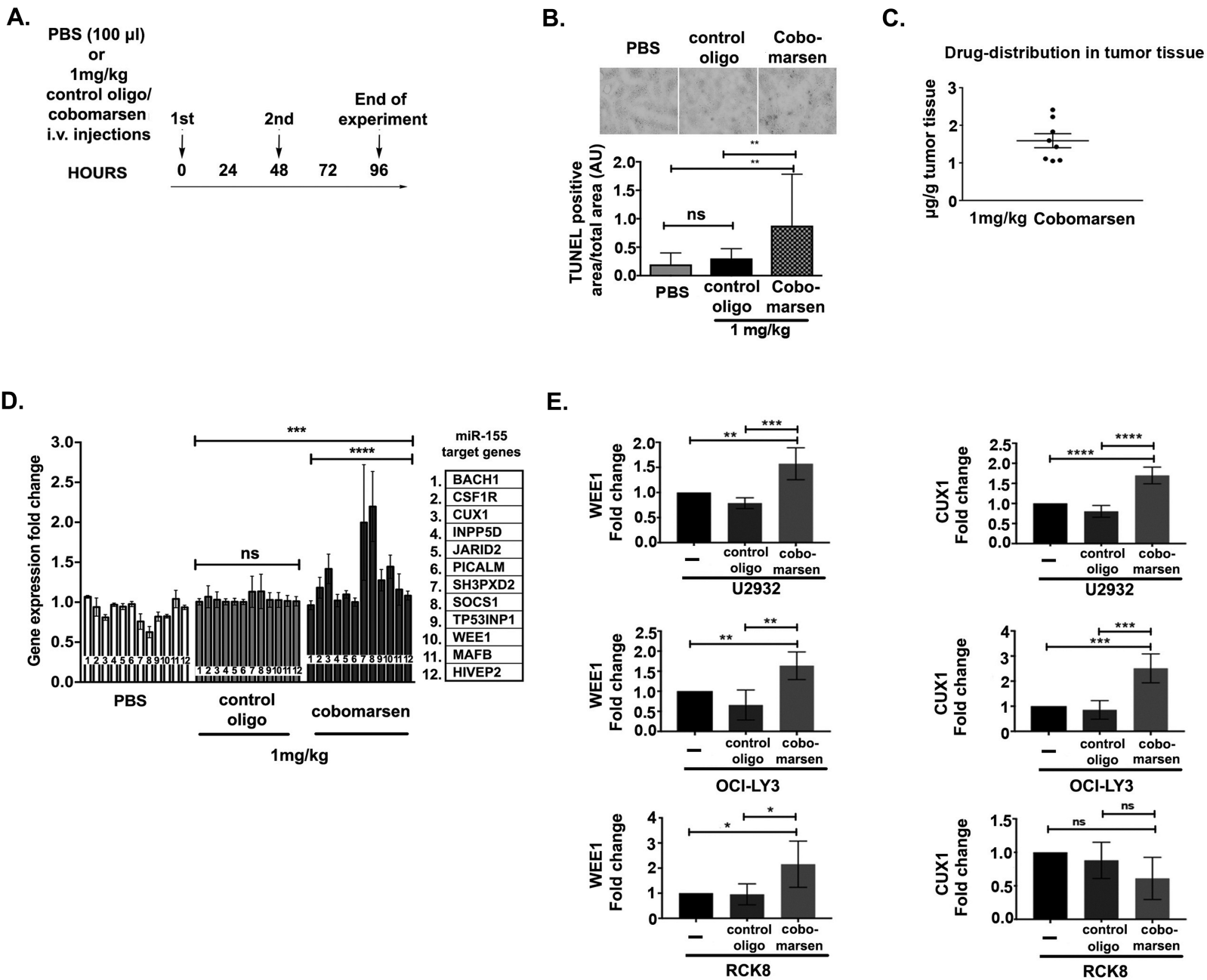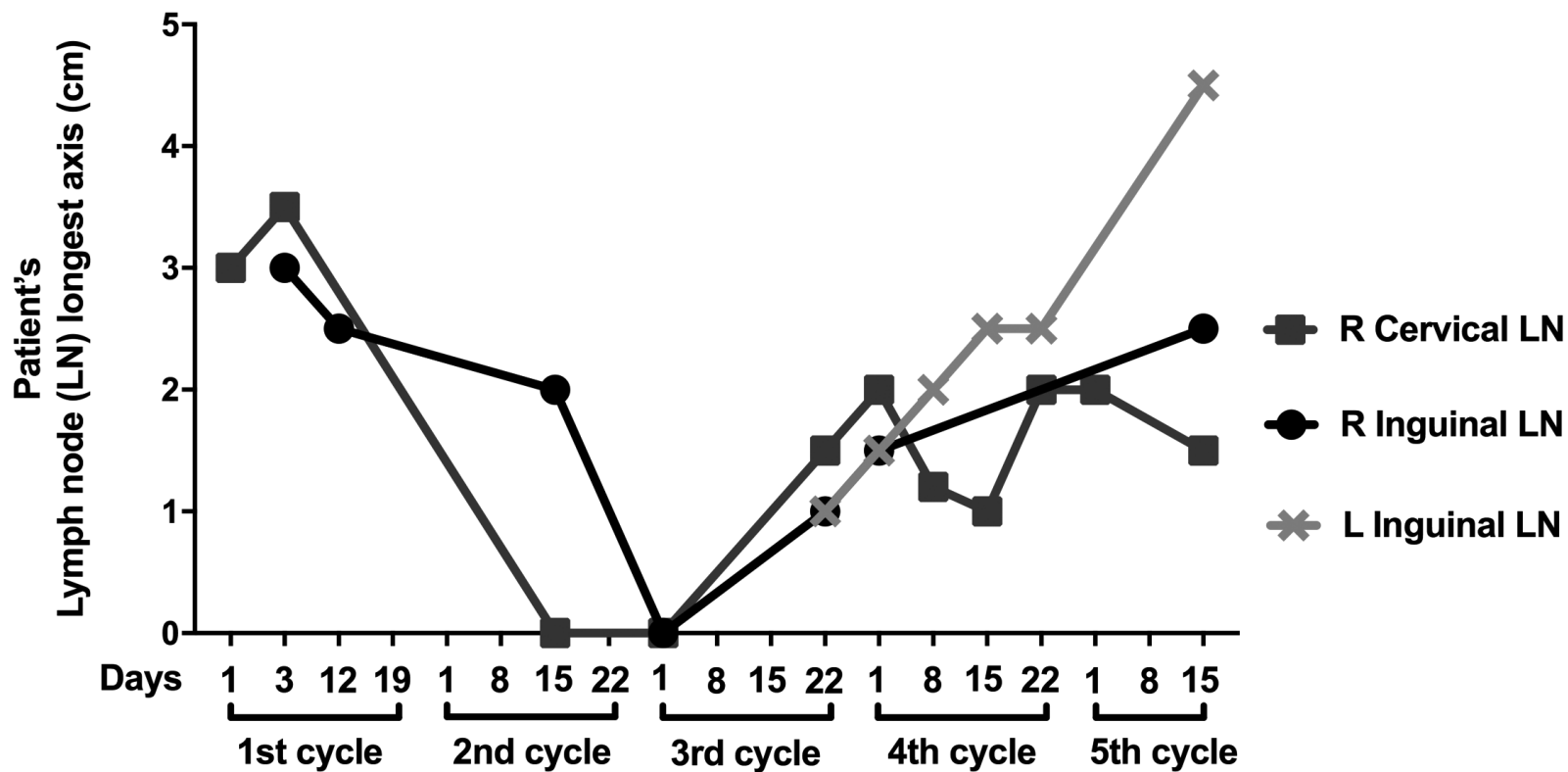
Clinical Cancer Research

Cobomarsen, an oligonucleotide inhibitor of miR-155, slows DLBCL tumor cell growth *in vitro* and *in vivo*

Eleni ANASTASIADOU, Anita Seto, Xuan Beatty, et al.

Updated version	Access the most recent version of this article at: doi:10.1158/1078-0432.CCR-20-3139
Supplementary Material	Access the most recent supplemental material at: http://clincancerres.aacrjournals.org/content/suppl/2020/11/18/1078-0432.CCR-20-3139.DC1
Author Manuscript	Author manuscripts have been peer reviewed and accepted for publication but have not yet been edited.

E-mail alerts	Sign up to receive free email-alerts related to this article or journal.
Reprints and Subscriptions	To order reprints of this article or to subscribe to the journal, contact the AACR Publications Department at pubs@aacr.org.
Permissions	To request permission to re-use all or part of this article, use this link http://clincancerres.aacrjournals.org/content/early/2020/11/18/1078-0432.CCR-20-3139. Click on "Request Permissions" which will take you to the Copyright Clearance Center's (CCC) Rightslink site.